

# Supporting Information

## Influence of the Synthesis Protocol on the Catalytic Performance of PHI-Type Zeolites for the Dehydration of Lactic Acid

Dorothea Häussermann, Richard Schömig, Barbara Gehring and Yvonne Traa\*

Institute of Technical Chemistry, University of Stuttgart, 70550 Stuttgart, Germany.

\* Correspondence: yvonne.traa@itc.uni-stuttgart.de.

### 1. Catalytic Performance of the Catalysts over TOS

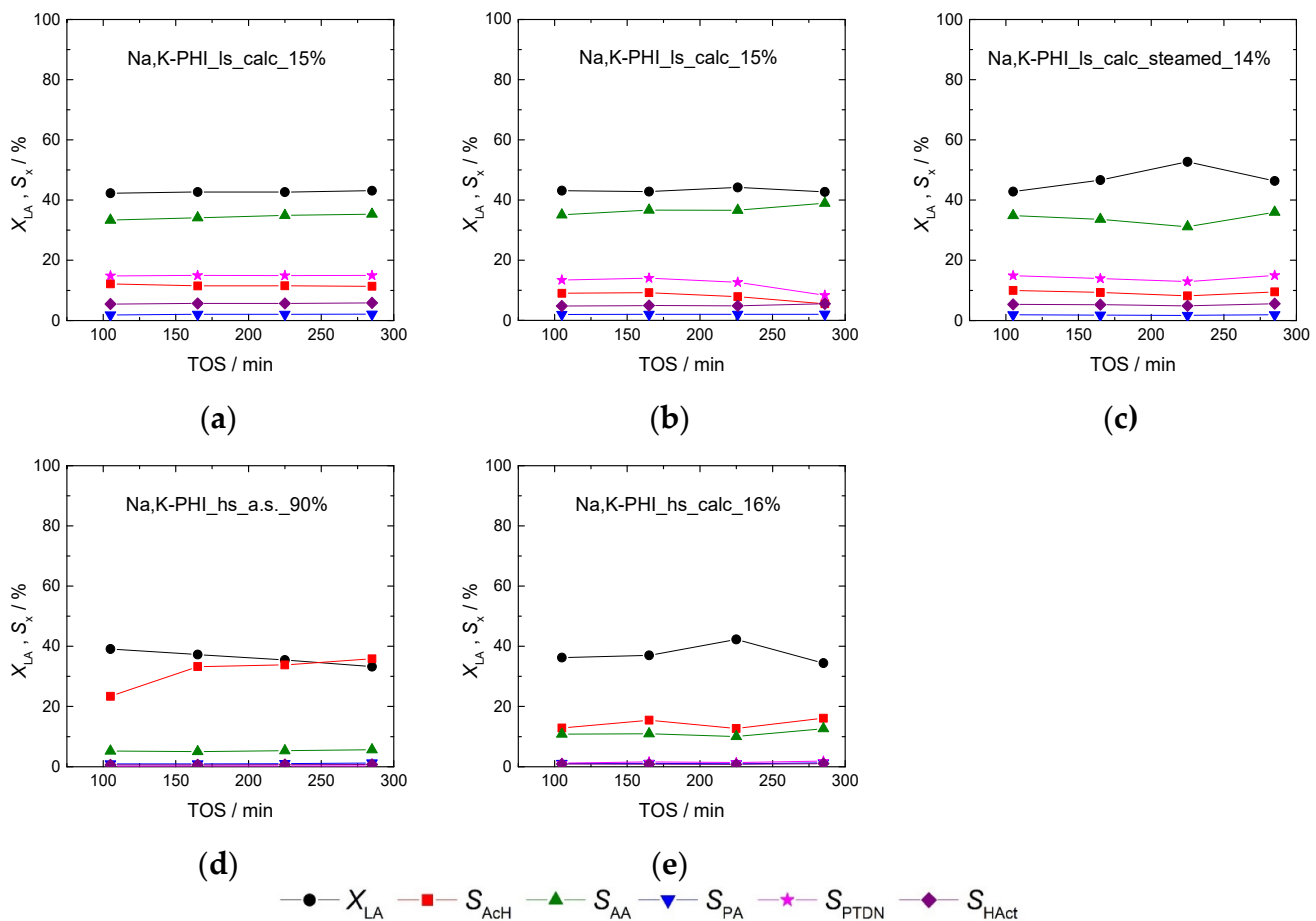


**Figure S1.** Catalytic performance of the catalysts. Conversion of lactic acid  $X_{LA}$  and selectivities to acrylic acid  $S_{AA}$ , acetaldehyde  $S_{AcH}$ , propionic acid  $S_{PA}$ , 2,3-pentanedione  $S_{PTDN}$  and hydroxyacetone  $S_{HAct}$  as a function of time-on-stream TOS. Na,K-PHI\_ls\_calc\_15% was measured twice freshly (a+b). Thus the reproducibility of the measurements is demonstrated. Na,K-PHI\_ls\_calc\_steam\_14% (c), Na,K-PHI\_hs\_a.s.\_90% (d) and Na,K-PHI\_hs\_calc\_16% (e) were measured once. The lines are interpolations to guide the eye. Reaction conditions: 0.5 g catalyst, LHSV = 3 h<sup>-1</sup>, 598 K.

## 2. CO<sub>2</sub> Physisorption Isotherms

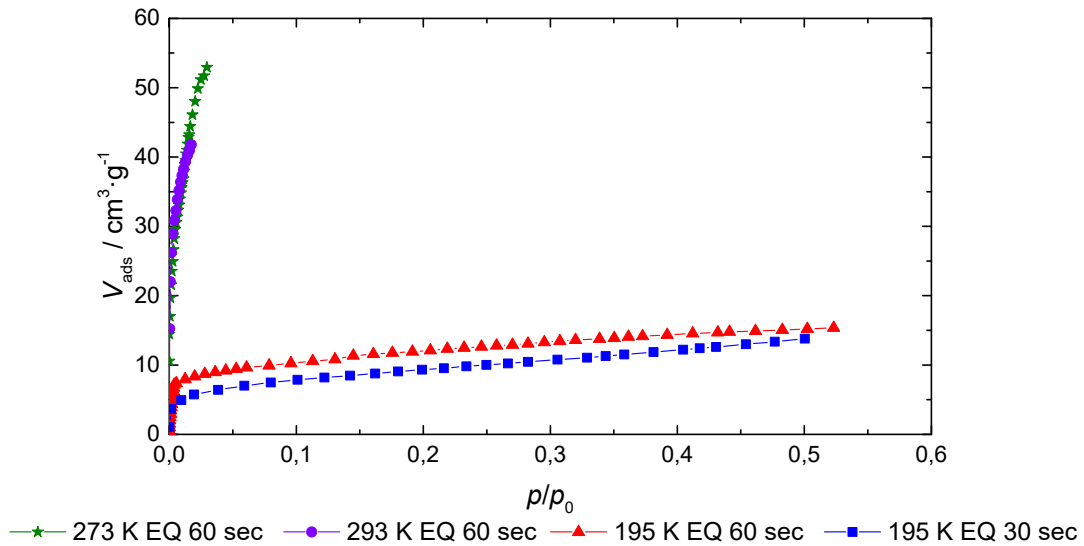


**Figure S2.** CO<sub>2</sub> physisorption isotherms for Na,K-PHI\_hs\_a.s.\_90% at 273 K and 195 K and different equilibration times (EQ). At 195K, the kinetic inhibition is clearly visible.

## 3. Pore Size Distributions

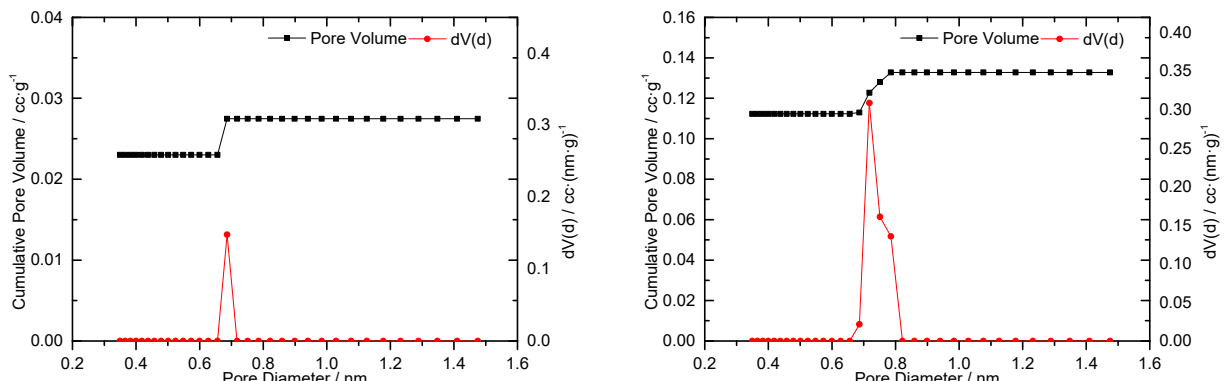


**Figure S3.** Pore size distributions calculated with Grand Canonical Monte Carlo Simulation (CO<sub>2</sub> at 273 K on carbon (GCMC model)) for the CO<sub>2</sub> physisorption measurements at 273 K for Na,K-PHI\_hs\_a.s.\_90% (left) and Na,K-PHI\_hs\_calc\_16% (right). The fitting error for Na,K-PHI\_hs\_a.s.\_90% was 18.359 % and for Na,K-PHI\_hs\_calc\_16% was 3.832 %.

#### 4. $^{27}\text{Al}$ MAS NMR Spectra of the Hydrated Zeolites

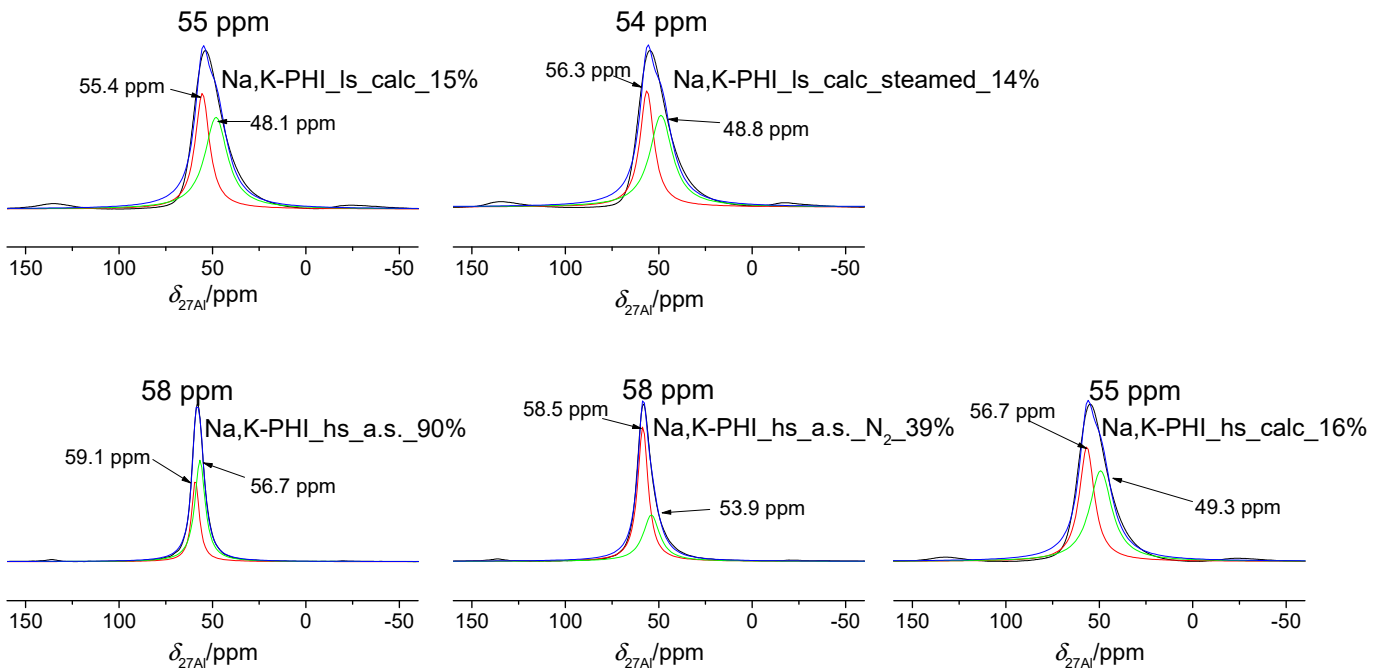


**Figure S4.**  $^{27}\text{Al}$  MAS NMR spectra of the hydrated zeolites. Experimental spectra (black) and mathematically deconvoluted spectra using Lorentzian lines (red and green) and overall mathematical fit (blue).

#### 5. Carbon Contents of the Catalysts after the Reaction

**Table S1.** Carbon content  $w_c$  of the catalysts after the reaction.

	Na,K-PHI_ls_calc_15%	Na,K-PHI_ls_calc_steam_14%	Na,K-PHI_hs_a.s._90%	Na,K-PHI_hs_calc_16%
$w_c$ / wt.-%	1.2	1.3	0.5	0.4

#### 6. Calculation of the Size of the Lactic Acid Molecule

The molecule size was investigated by density functional theory (DFT) and the semi-empirical GFN2-xTB [42] method. All DFT calculations were performed in Turbomole V7.4.1 [43] in ChemShell [44,45] via DL-FIND [46]. After initial optimization at the GFN2-xTB level, subsequent use of the Conformer Rotamer Ensemble Sampling Tool (CREST) [47] resulted in various conformers at the GFN2-xTB level. For these conformers, geometry optimizations were performed at the B3LYP-D3(BJ)/def2-SVP level followed by a single-point energy calculation of the optimized geometry at M06/def2-TZVP level. For all DFT-optimized structures, the molecule sizes were determined as the smallest diameter of a cylinder through which the rigid ligand would fit. Each atom is delimited by its van-der-Waals radius. The analysis was performed visually in VMD [48]. This procedure is analogous to the one described in Rieg et al. [49][50].

## References

42. Bannwarth, C.; Ehler, S.; Grimme, S. GFN2-xTB—An Accurate and Broadly Parametrized Self-Consistent Tight-Binding Quantum Chemical Method with Multipole Electrostatics and Density-Dependent Dispersion Contributions. *J. Chem. Theory Comput.* **2019**, *15*, 1652–1671. <https://doi.org/10.1021/acs.jctc.8b01176>.
43. A Development of University of Karlsruhe and Forschungszentrum Karlsruhe GmbH, 1989–2007, Turbomole V7.4.1 2019; TURBOMOLE GmbH: Karlsruhe, Germany, 2007.
44. Sherwood, P.; de Vries, A.H.; Guest, M.F.; Schreckenbach, G.; Catlow, C.R.A.; French, S.A.; Sokol, A.A.; Bromley, S.T.; Thiel, W.; Turner, A.J.; et al. QUASI: A general purpose implementation of the QM/MM approach and its application to problems in catalysis. *J. Mol. Struct. THEOCHEM* **2003**, *632*, 1–28. [https://doi.org/10.1016/S0166-1280\(03\)00285-9](https://doi.org/10.1016/S0166-1280(03)00285-9).
45. Metz, S.; Kästner, J.; Sokol, A.A.; Keal, T.W.; Sherwood, P. ChemShell—A modular software package for QM/MM simulations. *WIREs Comput. Mol. Sci.* **2014**, *4*, 101–110. <https://doi.org/10.1002/wcms.1163>.
46. Kästner, J.; Carr, J.M.; Keal, T.W.; Thiel, W.; Wander, A.; Sherwood, P. DL-FIND: An Open-Source Geometry Optimizer for Atomistic Simulations. *J. Phys. Chem. A* **2009**, *113*, 11856–11865. <https://doi.org/10.1021/jp9028968>.
47. Pracht, P.; Bohle, F.; Grimme, S. Automated exploration of the low-energy chemical space with fast quantum chemical methods. *Phys. Chem. Chem. Phys.* **2020**, *22*, 7169–7192. <https://doi.org/10.1039/C9CP06869D>.
48. Humphrey, W.; Dalke, A.; Schulten, K. VMD—Visual Molecular Dynamics. *J. Mol. Graph.* **1996**, *14*, 33–38. [https://doi.org/10.1016/0263-7855\(96\)00018-5](https://doi.org/10.1016/0263-7855(96)00018-5).
49. Rieg, C.; Dittmann, D.; Li, Z.; Lawitzki, R.; Gugeler, K.; Maier, S.; Schmitz, G.; Kästner, J.; Estes, D.P.; Dyballa, M. Quantitative Distinction between Noble Metals Located in Mesopores from Those on the External Surface. *Chem. Eur. J.* **2021**, *27*, 17012–17023. <https://doi.org/10.1002/chem.202102076>.
50. Rieg, C.; Kirchhof, M.; Gugeler, K.; Beurer, A.-K.; Stein, L.; Dirnberger, K.; Frey, W.; Bruckner, J.R.; Traa, Y.; Kästner, J.; Ludwigs, S.; Laschat, S.; Dyballa, M. Determination of Accessibility and Spatial Distribution of Chiral Rh Diene Complexes Immobilized on SBA-15 via Phosphine-based Solid-State NMR Probe Molecules. *Catal. Sci. Technol.* **2023**, *13*, 410–425. <https://doi.org/10.1039/d2cy01578a>.